

The Fock-Darwin States of Dirac Electrons in Graphene-based Artificial Atoms

Hong-Yi Chen*, Vadim Apalkov†, and Tapash Chakraborty*

*Department of Physics and Astronomy, University of Manitoba, Winnipeg, MB R2T 2N2, Canada

†Department of Physics and Astronomy, Georgia State University, Atlanta, Georgia 30303, USA

We have investigated the Fock-Darwin states of the massless chiral fermions confined in a graphitic parabolic quantum dot. In the light of the Klein tunneling, we have analyzed the condition for confinement of the Dirac fermions in a cylindrically-symmetric potential. New features of the energy levels of the Dirac electrons as compared to the conventional electronic systems are discussed. We have also evaluated the dipole-allowed transitions in the energy levels of the dots. We propose that in the high magnetic field limit, the band parameters can be accurately determined from the dipole-allowed transitions.

PACS numbers: 81.05.Uw, 73.63.Kv, 73.63.-b

Quantum dots (QDs), or the ‘artificial atoms’ [1] are one of the most intensely studied systems in condensed matter physics where the fundamental effects related to various quantum phenomena in confined geometries can be studied but with the unique advantage that the nature of the confinement and the electron density can be tuned externally. However, much of the interest on this system derives from its enormous potentials for applications, ranging from novel lasers to quantum information processing. While the majority of the QD systems investigated are based on the semiconductor heterostructures, in recent years, quantum dots created in the carbon nanotubes have been reported in the literature where the ‘atomic’ properties [2] were clearly elucidated and its importance in technological applications was also demonstrated [3]. Conductance properties of ultrathin graphitic QDs [4] have also been reported recently. It is now well recognized that the low-energy dynamics of the two-dimensional electrons in graphene is governed by the Dirac-Weyl equation, and the charge carriers behave as massless chiral fermions [5, 6]. In this situation, confinement of electrons becomes quite a challenging task, due to the so-called Klein’s paradox [7]. This problem has been dealt with in the case of a one-dimensional (1D) wire in zero [8] and in finite [9] magnetic fields. In this letter, we report on the electronic properties of the parabolic QDs in graphene, in particular, we present the energy levels as a function of the magnetic field (Fock-Darwin states [1]) and the associated dipole-allowed optical transitions in this system. We propose that the optical spectroscopy of the graphene QD in the high-field limit could provide an accurate means of determining the band parameters of graphene.

The Hamiltonian of a single electron in graphene with a cylindrically symmetric confinement potential is

$$\mathbf{H} = \mathbf{H}_0 + \mathbf{H}_1 = \frac{\gamma}{\hbar} (\vec{\sigma} \vec{\pi}) + V(r), \quad (1)$$

where $\vec{\sigma}$ are the Pauli matrices, $\vec{\pi} = \vec{p} + \frac{e}{c} \vec{A}$, $\vec{A} = \frac{B}{2}(-y, x)$ is the vector potential corresponding to the magnetic field B in the z -direction orthogonal to the

graphene plane, and $\gamma = \sqrt{3}a\gamma_0/2$ is the band parameter. Here $a = 0.246$ nm is the lattice constant and γ_0 (meV) is the transfer integral between the nearest-neighbor carbon atoms [10].

At first we analyze the properties of the graphene system in the absence of a magnetic field to find the condition for confinement of an electron in the potential $V(r)$. Due to the Klein tunneling the electrons in graphene can not be localized by a confinement potential, since for any potential there will be the electron states with negative energy (the hole states) which would provide the escape channel for the electron inside the potential well. We can then discuss only the quasilocalized states or trapping of the electron by the confinement potential. This problem has been treated for the quasi-1D graphene system [8, 11], where it was shown that the transverse momentum in 1D introduces the classically forbidden regions, which helps in trapping the electron. The width of the quasilocalized level is determined by the tunneling through the classically forbidden regions. For the zero transverse momentum, the tunneling barriers disappear and there are no trapped states. In our case, we have a cylindrically symmetric confinement potential with the effective transverse momentum m/r , where m is the electron angular momentum. Therefore, for $m \neq 0$ we expect the trapping of an electron by a cylindrically symmetric QD. In terms of the two-component wave function ($\chi_1(r)e^{i(m-1)\theta}$, $\chi_2(r)e^{im\theta}$) the Schrödinger equation corresponding to the Hamiltonian (1), is

$$V(r)\chi_1 - i\gamma \frac{d\chi_2}{dr} - i\gamma \frac{m}{r}\chi_2 = E\chi_1 \quad (2)$$

$$V(r)\chi_2 - i\gamma \frac{d\chi_1}{dr} + i\gamma \frac{m-1}{r}\chi_1 = E\chi_2. \quad (3)$$

There are no analytical solution to these equations, and therefore, we first present below a semiclassical analysis.

Semiclassical analysis: At a large m we seek a solution of Eqs. (2)-(3) in the form e^{iqr} , which gives

$$\left(\frac{E-V}{\gamma}\right)^2 = \left(\frac{m}{r}\right)^2 + q^2. \quad (4)$$

The classical turning points can be found from the condition $q = 0$, and the classical region is $|E - V(r)| > \gamma|m|/r$. If r_0 is the solution of the equation $E - V(r) = 0$ then we can find the classically forbidden region as $(r_0 - \Delta r) < r < (r_0 + \Delta r)$, where $\Delta r = m/Fr_0$, $F = \gamma^{-1}dV(r_0)/dr$, and we assumed that $F \gg m/r_0^2$. If the electron is trapped in the dot, i.e., at $r < r_0 - \Delta r$, then the escape rate or the width of the quasilocalized levels is determined by the tunneling through the classically forbidden region,

$$T = \exp \left(- \int_{r_0 - \Delta r}^{r_0 + \Delta r} |q(r)| dr \right) = \exp \left(- \frac{\pi m^2}{2Fr_0^2} \right). \quad (5)$$

Therefore, in order to trap the electron we need a large m and a small F , i.e. a smooth confinement potential. For a potential $V = (u/n)r^n$, Eq. (5) takes the form

$$T = \exp \left[- \frac{\pi \gamma m^2}{2ur_0^{n+1}} \right] = \exp \left[- \frac{\pi m^2}{n(E/\epsilon_n)^{n+1/n}} \right], \quad (6)$$

where $\epsilon_n = (\gamma^n u/n)^{1/(n+1)}$. Equation (6) gives the upper limit on the energy of the quasilocalized levels at a given m , i.e. $E/\epsilon_n < m^{2n/(n+1)}$. Based on the semiclassical expression we can also find the interlevel separation of the quasilocalized levels at large energies, $\Delta E_n = \alpha \epsilon_n (E/\epsilon_n)^{-1/n}$, where $\alpha \sim 1$. We then estimate the number of quasilocalized levels, $N_{n,m}$ for a given angular momentum, m , and a given potential profile from

$$N_{n,m} = \int_0^{m^{2n/(n+1)}} \frac{dE}{\Delta E_n} \sim \frac{n}{n+1} m^2. \quad (7)$$

This estimation is valid for a large m . For a small m we need to solve the system of equations (2)-(3) numerically to find the properties of the quasilocalized states.

Quasilocalized states – numerical solutions: To extract the information about the width of the quasibound levels we need to impose special boundary conditions far from the QD. This condition means that far from the origin, $r \gg r_0$, the solution should be an outgoing wave, i.e., the propagation away from the QD. From Eqs. (2)-(3), it is clear that for $r \gg r_0$ the outgoing solution has the form

$$\chi_1(r) = -\chi_2(r) = C \exp \left(\frac{i}{\gamma} \int^r V(r') dr' \right), \quad (8)$$

where C is a constant. Equation (8) is the boundary condition for the system (2)-(3) at large distances. Since at $r = 0$ the solution should be non-divergent, another boundary condition is $\chi_1(r = 0) = \chi_2(r = 0) = 0$. A solution with these boundary conditions exists only for a complex energy, E . The imaginary part of the energy determines the width of the quasilocalized level.

We have solved Eqs. (2)-(3) numerically for a potential of the form $V(r) = (\frac{u}{n})r^n$ with different values of the exponent, n , and for different values of the angular momentum m . In the dimensionless units, i.e., for the

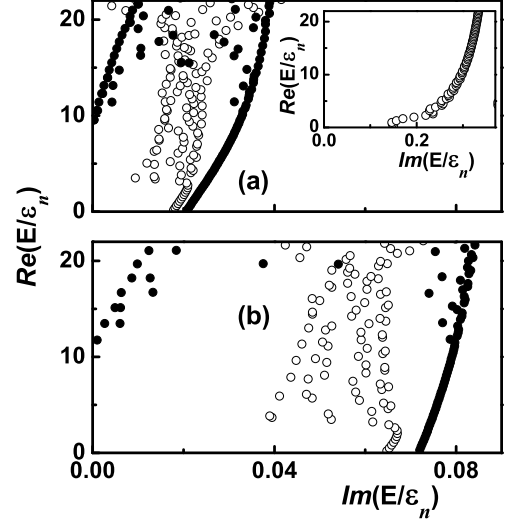


FIG. 1: The real and imaginary parts of the energy spectra of an electron in a QD with a confinement potential $V(r) = (u/n)r^n$, shown for various values of the exponent n and the angular momentum m : (a) $n = 2$, $m = 2$ (circles), and $n = 2$, $m = 10$ (dots); (b) $n = 4$, $m = 2$ (circles), and $n = 4$, $m = 10$ (dots). The results for $n = 2$ and $m = 1$ are shown as inset. The energy is in units of ϵ_n .

units of length and the energy, $a_n = (n\gamma/u)^{1/(n+1)}$ and $\epsilon_n = (\gamma^n u/n)^{1/(n+1)}$ respectively, the system does not contain any information about the interaction strength, u . The results in Fig. 1 show a bunch of closely spaced levels with a large imaginary part of the energies, $\text{Im}(E)$. For these states $\text{Im}(E)$ is comparable to the interlevel spacing. These states are the delocalized continuum states. At the background of the continuum spectra we also see the levels with a small imaginary energy, i.e. a small width of the level. These states are the quasilocalized states of the QD. The manifestation of such states can be seen already at $m = 2$ (circles) both for $n = 2$ [Fig. 1(a)] and $n = 4$ [Fig. 1(b)]. The strength of the localization can be characterized in terms of the ratio of the $\text{Im}(E)$ to the interlevel spacing. For $m = 2$ this ratio is 50. With an increase of the magnetic moment the quasilocalized states become well developed and at $m = 10$ we clearly see the states with very low $\text{Im}(E)$. The ratio of $\text{Im}(E)$ to the interlevel spacing for these states is about 800. With an increase of the energy the states are less localized, i.e. $\text{Im}(E)$ increases. This is consistent with Eq. (6). Note that for all values of the exponent n there are no localized states at $m = 1$ [inset in Fig. 1(a)]. All the states at $m = 0$ have very large $\text{Im}(E)$. There are also no quasilocalized states at $m = 0$. The reason for delocalization of the electron at $m = 0$ and 1 is that the effective transverse momentum for either the χ_1

component (at $m = 0$) or the χ_2 component (at $m = 1$) is zero. In the following, we analyze the magnetic field effects on the electronic states of the QDs.

Magnetic Field – semiclassical analysis: In a magnetic field the system of equations (2)-(3) has an additional non-diagonal term proportional to the magnetic field. In the dimensionless units, i.e., for the units of length a_n and the energy ϵ_n , the system is characterized by only one parameter, $b = (eB/2c)(n\gamma/u)^{2/(n+1)}$. In the semiclassical approximation, the effective transverse momentum is $(m/r + br)$ and the Eq. (4) becomes

$$T = \exp \left[-\frac{\pi(m + b\tilde{E}^{2/n})^2}{n\tilde{E}^{n+1/n}} \right], \quad (9)$$

where $\tilde{E} = E/\epsilon_n$. The effect of the magnetic field is different for the states with a positive or a negative m (the sign of m depends on the direction of a magnetic field). For a positive m the application of a magnetic field increases the effective transverse momentum and suppresses the tunneling from the QD. For a negative m , the magnetic field *decreases* the transverse momentum. Therefore the state becomes less localized. If we increase the magnetic field even further then at some point, $b = m/\tilde{E}^{2/n}$, the level becomes *delocalized*, and at a even larger B the level again becomes localized. Now the trapping will be due to the magnetic field. Therefore for a negative m , the magnetic field induces a *localization-delocalization-localization* transition.

The number of the quasilocalized states in a weak magnetic field is estimated to be $N_{n,m} \sim [m + b|m|^{2/(n+1)}]^2$. This number with a positive m increases with an increasing magnetic field, while that for a negative m decreases with the magnetic field upto a certain value of B and then increases. The total number of states with positive and negative angular momenta, $N_{n,m} + N_{n,-m} \sim m^2 + b^2|m|^{4/(n+1)}$ always increases with an increasing B . From this behavior we expect the following effect: We assume that the QD is occupied by electrons upto a certain energy, i.e., the states with both positive and negative angular momenta are occupied and the net angular momentum of the dot is zero. We then apply a magnetic field and the states with positive m becomes more localized while the electrons from the states with negative m will escape from the QD. Finally, the electrons in the QD will have a net positive angular momentum and correspondingly a net magnetic moment.

Magnetic Field – numerical results: To study the dependence of the quasilocalized spectra on the magnetic field we introduce the wavefunctions of the Hamiltonian \mathbf{H}_0 , i.e. without a confinement potential [12], as the basis functions. To eliminate any escape of the electron from the QD we consider only the basis functions with the positive energy,

$$\Psi_{n,m} = C_N \begin{pmatrix} \text{sgn}(N)\phi_{n,m-1}(x) \\ i\phi_{n,m}(x) \end{pmatrix}, \quad (10)$$

where $N = n + \frac{1}{2}(|m| + m)$ is the Landau Level (LL) index, $C_{N=0} = 1$ and $C_{N \neq 0} = 1/\sqrt{2}$, $\text{sgn}(N = 0) = 0$, and

$$\phi_{n,m} = \frac{1}{\sqrt{2}} \sqrt{\frac{n!}{(n+|m|)!}} e^{-x/2} x^{|m|/2} L_n^{|m|}(x) e^{im\theta} \quad (11)$$

is the Landau wavefunction. Here $L_n^{|m|}(x)$ is the associated Laguerre polynomial, $x = r^2/a'^2$ is a dimensionless distance. Here a' is the characteristic length of the system. Without the confinement a' should be equal to the magnetic length $l = \sqrt{\hbar c/eB}$. In the presence of the confinement, the Hamiltonian suggests a natural unit of length $(\gamma/u)^{1/3}$ [8] and a natural unit of energy $(\gamma^2 u)^{1/3}$. This length characterizes the size of a parabolic dot in graphene. Therefore,

$$\frac{2}{a'^2} = \frac{1}{l^2} + \left(\frac{u}{\gamma}\right)^{2/3}.$$

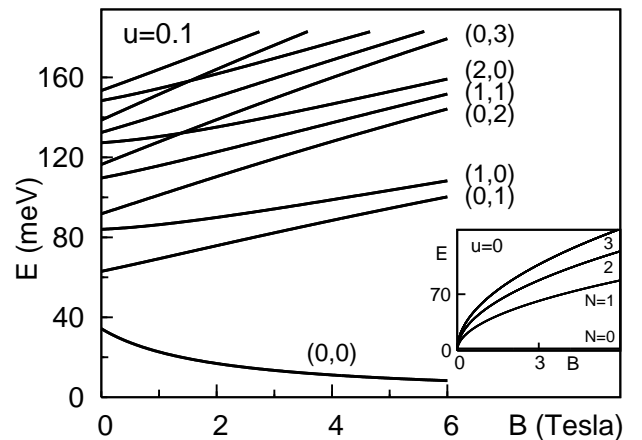


FIG. 2: Fock-Darwin spectrum of the Dirac quantum dots, plotted for the confinement potential strength $u = 0.1$ (in dimensionless units). The numbers in the parentheses correspond to the two quantum numbers n and m . Results for $u = 0$ are given as an inset.

In our numerical calculations, we choose the band parameter to be $\gamma = 646$ meV·nm for $\gamma_0 = 3.03$ eV [13]. The low-lying energy states of the graphene QD are shown in Fig. 2. In the absence of a confinement potential, the Dirac spectrum scales as $\sqrt{2}\gamma\sqrt{N}/l$ [shown as inset]. In the Fock-Darwin spectrum for a conventional electron dot, the energy levels are degenerate and equally spaced at $B = 0$ [1]. The two-dimensional parabolic confinement considered here shows two outstanding features in contrast to the Fock-Darwin spectra at $B = 0$. The first is the lifting of the degeneracy and the other is the unequal separation among the energy levels. Figure 2 shows the field-dependent energy spectrum for $u = 0.1$. The energy difference between the lowest two levels at $B = 0$ is about $(\gamma^2 u)^{1/3}$. At a low magnetic field, the

magnetic length l is larger than or comparable to the size of the confinement $(\gamma/u)^{1/3}$ and there is a hybridization of the LLs with the levels arising from the spatial confinement. In the high magnetic field limit $l \ll (\gamma/u)^{1/3}$, the Landau-type levels prevail, as expected. The Fock-Darwin spectra for conventional quantum dots have been determined earlier by the transport spectroscopy [14]. Similar studies for the graphene QDs would be very important to explore the energy levels and the nature of confinement for Dirac fermions in a graphene QD.

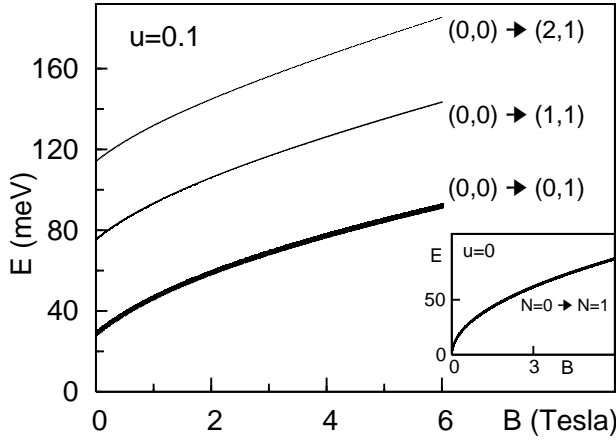


FIG. 3: The dipole-allowed transitions in the Fock-Darwin spectrum of graphene QDs for $u = 0.1$. Inset: the case of $u = 0$. The thickness of the lines is proportional to the calculated intensity. From the bottom to the top, the relative intensities are about 1.0, 0.1, 0.02, respectively.

Figure 3 shows the dipole-allowed optical absorption spectra [1, 15] for $u = 0$ and $u = 0.1$. Without any confinement there is only the $(0,0) \rightarrow (0,1)$ transition (shown as inset in Fig. 3). The additional transitions, $(0,0) \rightarrow (1,1)$ and $(0,0) \rightarrow (2,1)$ are due to the presence of the parabolic confinement. For the Dirac fermions in a QD, the lowest dipole-allowed transition is

$$\Delta E \simeq (\gamma^2 u)^{1/3} + \frac{\sqrt{2}\gamma}{l}. \quad (12)$$

For $B = 0$ the corresponding energy is $\approx (\gamma^2 u)^{1/3}$. As the magnetic field increases, ΔE approaches the cyclotron energy $\sqrt{2}\gamma/l = \sqrt{2}(e\gamma B/\hbar c)$, where γ can therefore be uniquely determined experimentally. Conventionally, in the nearest-neighbor tight-binding model, γ_0 is obtained by fitting the *ab initio* calculation and the experimental data [10]. In a GaAs quantum dot, the magnetic-field-dependent far-infrared absorption experiments have established the energy relation $\Delta E_{\pm} = \hbar\Omega \pm \frac{1}{2}\hbar\omega_c$ to a great accuracy [15]. Similarly, for the massless chiral fermions in a graphene QD, we expect that the band pa-

rameter γ can also be determined quite accurately by the optical absorption experiments in the high-field limit.

Although the high magnetic field results are the major focus of this paper as in this case the localization of the electron in a QD at all values of the m is provided by the magnetic field, at $B=0$ the chiral nature of the states prevent the electrons from being confined in a QD. This clearly indicates that the nature of the energy states and the optical spectra at a very small B are still important open questions.

We would like to thank P. Pietiläinen and Xue-Feng Wang for helpful discussions. The work has been supported by the Canada Research Chair Program and a Canadian Foundation for Innovation Grant.

-
- [1] T. Chakraborty, *Quantum Dots* (Elsevier, Amsterdam, 1999); T. Chakraborty, *Comments Condens. Matter Phys.* **16**, 35 (1992).
 - [2] M.R. Buitelaar et al., *Phys. Rev. Lett.* **88**, 156801 (2002); D.H. Cobden, and J. Nygård, *ibid.* **89**, 046803 (2002); S. Moriyama et al., *ibid.* **94**, 186806 (2005); S.-H. Ke, H.U. Baranger, and W. Yang, *ibid.* **91**, 116803 (2003).
 - [3] K. Ishibashi et al., *J. Vac. Sci. Technol. A* **24**, 1349 (2006).
 - [4] J. Scott Bunch et al., *Nano Lett.* **5**, 287 (2005).
 - [5] K.S. Novoselov et al., *Nature* **438**, 197 (2005); Y. Zhang et al., *ibid.* **438**, 201 (2005).
 - [6] T. Ando, in *Nano-Physics & Bio-Electronics: A New Odyssey*, edited by T. Chakraborty, F. Peeters, and U. Sivan (Elsevier, Amsterdam, 2002), Chap. 1.
 - [7] M.I. Katsnelson, K.S. Novoselov, and A.K. Geim, *Nature Phys.* **2**, 620 (2006); O. Klein, *Z. Phys.* **53**, 157 (1929); **41**, 407 (1927); A. Calogeracos and N. Dombey, *Contemp. Phys.* **40**, 313 (1999).
 - [8] P.G. Silvestrov and K.B. Efetov, cond-mat/0606620 (unpublished).
 - [9] N.M.R. Peres, A.H. Castro Neto, and F. Guinea, *Phys. Rev. B* **73**, 241403 (2006).
 - [10] R. Saito, G. Dresselhaus, and M.S. Dresselhaus, *Physical Properties of Carbon nanotubes* (Imperial College Press, London, 1998).
 - [11] V. V. Cheianov and V. I. Falko, *Phys. Rev. B* **74**, 041403 (2006).
 - [12] Y. Zheng and T. Ando, *Phys. Rev. B* **65**, 245420 (2002).
 - [13] T. Ando, *J. Phys. Soc. Jpn.* **75**, 074716 (2006).
 - [14] P.L. McEuen et al., *Phys. Rev. Lett.* **66**, 1926 (1991); J. Weis et al., *Phys. Rev. B* **46**, 12837 (1992); T. Schmidt et al., *ibid.* **51**, 5570 (1995); S. Tarucha et al., *Phys. Rev. Lett.* **77**, 3613 (1996).
 - [15] C. Sikorski and U. Merkt, *Phys. Rev. Lett.* **62**, 2164 (1989); B. Meurer, D. Heitmann, and K. Ploog, *Phys. Rev. Lett.* **68**, 1371 (1992); D. Heitmann and J. Kotthaus, *Phys. Today* **46**, 56 (1993).